*Desalination and Water Treatment*
www.deswater.com

doi: 10.5004/dwt.2017.21092

81 (2017) 265–273
June

# Removal of textile dyes from aqueous solutions by lignin and its derivative charcoals: characterization, adsorption kinetics and isotherms

Maryam El Marouani[a], Laila El Fakir[a], Samir Men La Yakhaf[b], Nadia El Hrech[c], Abdelmalek Dahchour[d], Saloua Sebbahi[a,*], Souad El Hajjaji[a], Fatima Kifani-Sahban[e]

[a]*Laboratory of Spectroscopy, Molecular Modeling, Materials, Nanomaterials, water and Environment (LS3MN2E), Department of Chemistry, Faculty of Sciences, Mohamed V University, Av Ibn Battouta, B.P. 1014, Rabat 10000, Morocco, Tel. +212 6 61 39 79 64; emails: sebbahi_seloua@yahoo.fr (S. Sebbahi), maryam.elmarouani@gmail.com (M. El Marouani), laila_el@hotmail.fr (Laila El Fakir), selhajjaji@hotmail.com (S. El Hajjaji)*
[b]*Modeling and Simulation Laboratory of Mechanics and Energy (MSME), Physical Department, Faculty of Sciences, Mohamed V University, Av Ibn Battouta, B.P. 1014, Rabat 10000, Morocco, email: fsrsamiretm@gmail.com*
[c]*Laboratory of Nanostructures, Nanomaterials, Process Engineering and Environmental, Department of Chemistry, Faculty of Sciences, Mohamed V University, Av Ibn Battouta, B.P. 1014, Rabat 10000, Morocco, email: nelhrech@gmail.com*
[d]*Department of Fundamental and Applied Sciences, Hassan II Agronomic and Veterinary Institute, B.P. 62002, Rabat-Institute, Rabat 10000, Morocco, email: abdel_dahchour@yahoo.fr*
[e]*Laboratory of Thermodynamic and Energetic, Physical Department, Faculty of Sciences, Mohamed V University, Av Ibn Battouta, B.P. 1014, Rabat 10000, Morocco, email: kifani_sahban@yahoo.fr*

Received 30 November 2016; Accepted 1 July 2017

**ABSTRACT**

This work focuses on the adsorption in aqueous solution of methylene blue (MB) and methyl orange (MO) on raw lignin (RL), on its derivative charcoals (LC and ACL) and on commercial activated carbon (CAC) taken as reference. Derivative charcoals are the lignin char (LC) and the activated carbon of lignin (ACL). The adsorbents were characterized by infrared spectroscopy, transmission electron microscopy and specific surface area measurements. The optimum conditions determined using experimental designs are 50 mg of lignin, 5 mg/L of dye and 30 min contact time. The studied response is the retention rate. As regards the RL, MB is better adsorbed than MO. As for LC, the adsorption of MB and that of MO are equivalent but are significantly lower than on RL. On the other hand, with ACL, the adsorption of MB and that of MO are higher than those on RL and LC. Infrared analysis reveals that the responsible functional groups of adsorption are present in RL and in ACL, but not in LC. Besides, the specific surface area value of LC is significantly lower than those of RL and ACL. The adsorption of MB on ACL is comparable to that on CAC, while that of MO is higher. IR analysis showed the fixation of MB and MO on ACL. The adsorption process of the two dyes both on RL as on ACL is controlled by chemisorption and the two dyes are adsorbed in multilayers on heterogeneous surfaces.

*Keywords:* Lignin; Lignin char; Activated carbon of the lignin; Commercial activated carbon; Adsorption; Methylene blue; Methyl orange

## 1. Introduction

In our previous work, we had prepared an activated carbon from lignin by physical activation [1,2], certain assets of lignin were highlighted. It concerns its specific surface area and surface chemistry at raw and activated states, its thermal resistance and the yield of coal during carbonization [3]. Raw lignin (RL) has functional groups with adsorption character. Carbonization of lignin leads to mass loss [3] and to the elimination of most functional groups [2]. Carbonization is also accompanied by a plastic

* Corresponding author.

deformation with crazing. This is mainly shown through dimensional variations measurements and characterizations by scanning electron microscopy and infrared spectroscopy [2,3]. The formation of this phase slows the decomposition of lignin during carbonization leading to a good yield of coal [3]. Indeed, coal yield is of 50% at 700°C, significantly higher yield than that obtained after carbonization of cellulose and xylan. In addition, the plastic phase gives the thermal stability to charcoal during the activation and the oxidation decreases its thermal stability [1] and its activation time while improving surface chemistry and specific surface area [2]. All these advantages make our lignin and its activated carbon effective adsorbents to treat wastewater.

Otherwise, to our knowledge, the elimination of many types of pollutants in aqueous solution by RL and by its chars derived from chemical activation has already been the subject of many studies, which is not the case of chars derived from physical activation. Therefore, we are looking at in this work to examine the adsorption capacity of RL and of its derivative charcoals from the physical activation onto two most used dyes in the textile industry that are methylene blue (MB) and methyl orange (MO). These dyes are discharged directly into the aquatic environment without any prior treatment. In addition to their carcinogenic and genotoxic effects, the dyes released into the water reduce the penetration of light and have a negative effect on photosynthesis of aquatic plants [4]. Most of the dyes used are stable and are not biologically degradable.

## 2. Materials and experimental methods

### 2.1. Adsorbents

The adsorbents used in this work are RL, its derivative charcoals (LC and ACL) and commercial activated carbon (CAC) taken as reference. Derivative charcoals are the lignin char (LC) obtained after carbonization of lignin at 600°C for 2 h under nitrogen and the activated carbon of lignin (ACL) obtained by pre-oxidation of LC in air at 245°C for 6 h followed by gasification in the presence of carbon dioxide at 700°C for 30 min. These substrates are all employed in the powder state. Characteristics of RL and of its derivative charcoals as well as carbonization, pre-oxidation and activation procedures are given in a previous work [1].

### 2.2. Adsorbates

Examined adsorbates in this work are MB and MO which are two widely used dyes in textile industry. MB is an organic compound of chemical formula $C_{16}H_{18}N_3SCl$ (Fig. 1(a)). Its molecular mass is equal to 319.85 g/mol. It is an organic molecule belonging to the family of the xanthenes. It is a cationic dye $C_{16}H_{18}N_3S^+$ preferentially adsorbed by the acid sites of the adsorbent. This dye is selected as a representative model of organic pollutants of medium size. MO is an organic compound of chemical formula $C_{14}H_{14}N_3NaO_3S$ (Fig. 1(b)). Its molecular mass is of 327.33 g/mol. It is an anionic dye $C_{14}H_{14}N_3SO_3^-$ preferentially adsorbed by the basic sites of the adsorbents.

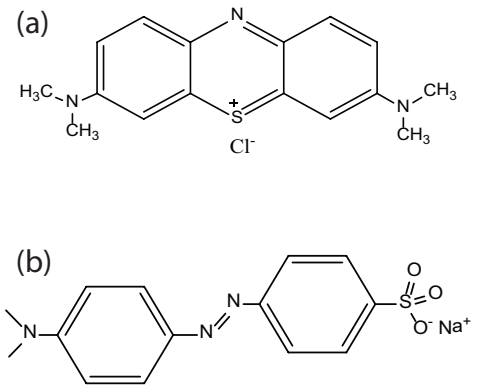


Fig. 1. Chemical structure of MB (a) and MO (b).

### 2.3. Adsorbents characterization

#### 2.3.1. Spectral characterization

The apparatus used for the characterization by infrared spectroscopy is a Bruker-Tensor 27, which operates in reflection mode. This apparatus is equipped with a Globar source that emits radiation in the region of mid-infrared and a DLaTGS detector. In the unity of attenuated total reflection (ATR), enough of the sample is placed, without prior preparation, on the crystal. In our analyses, the crystal used is the germanium crystal, which allows the acquisition between 4,000 and 600 $cm^{-1}$ in wave number. The number of scans is 20 with a resolution of 4 $cm^{-1}$. The device is controlled by OPUS software.

#### 2.3.2. Transmission electron microscope observation

The characterization by transmission electron microscope is done on a fine powder, using TECNAI G2/FEI equipment, high voltage (120 kV), provided with a CCD camera. The resolution is 0.35 nm and the enlargement varies from 150 to 500,000×.

#### 2.3.3. Measurement of surface charge of raw lignin

Measurement of surface charge is made into a suspension containing 0.1 g of RL and 100 mL of an aqueous solution of 0.1 M NaCl. Suspension is stirred for 2 h at room temperature, the corresponding initial pH being 6.25. The pH is then adjusted to a value of 2 by addition of 2 mL of 0.1 M HCl. The titration of the suspension is carried out by a solution of 0.01 M NaOH. The point of zero charge ($pH_{PZC}$), determined from the plot of the surface charge depending on the pH (Fig. 2), is equal to 2.25.

### 2.4. Experimental protocol of adsorption kinetics and isotherms

To follow the kinetics and the isotherms of adsorption of the two dyes on RL and on its derivative charcoals, the adsorbent is placed in 100 mL of a solution containing different concentrations of dye (2–10 mg/L). The mixture, at pH equal to 7, is subjected to stirring at room temperature and samples are taken every 5 min. The samples are followed by centrifugation and filtration. Absorbance is measured on a UV–visible spectrophotometer MAPADA 1600 type at

the wavelength related to maximum absorption of each dye (664 nm for MB and 464 nm for MO). The adsorbed amount ($q_e$) was calculated by the difference between the initial concentrations ($C_0$) and the equilibrium concentrations ($C_e$) using the relationship:

$$q_e = \frac{C_0 - C_e}{m} V \quad (1)$$

where $V$ and $m$ being, respectively, the volume in liters of the treated solution and the quantity in grams of the adsorbent.

The retention rate is then calculated as a function of the initial and equilibrium concentrations by the relation:

$$R\% = 100 \frac{C_0 - C_e}{C_0} \quad (2)$$

### 2.5. Methodology of experimental research

The methodology of experimental research (MER), based on experimental design [5,6], is used in this work to determine the optimal conditions of the parameters taken into consideration and to deduce the most influential factors. In our case, these parameters are the mass of the adsorbent, the initial concentration of the adsorbate and the contact time.

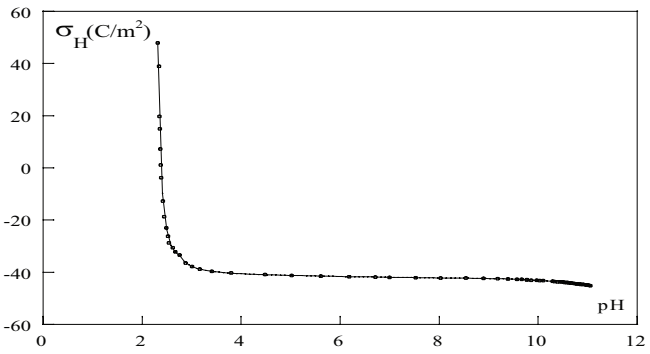


Fig. 2. Surface charge density of RL.

The full factorial matrix used is a $2^3$ matrix, which corresponds to eight tests in total. The experimental field for each parameter at two levels has been defined [high level (+1) and low level (–1)] [5,6]. Using the Nemrodw software [7], we were able to identify the most influential factors.

## 3. Results and discussion

### 3.1. Experimental study using the MER

The results obtained by performing the eight experiments of the $2^3$ full factorial plans are shown in Table 1. The retained optimal conditions are those corresponding to the highest retention rate. Thus, for the two dyes, the retention is maximal with 50 mg of lignin, 5 mg/L of dye and 30 min contact time (given in bold in Table 1).

If $Y$ is the response variable, then the regression equation with three parameters and their interaction is given by:

$$Y = b_0 + b_1 X_1 + b_2 X_2 + b_3 X_3 + b_{12} X_1 X_2 + b_{13} X_1 X_3 + b_{23} X_2 X_3 + b_{123} X_1 X_2 X_3$$

where $b_0$, $b_1$, $b_2$ and $b_3$ are the linear coefficients. $b_{12}$, $b_{13}$ and $b_{23}$ are the interaction terms of the second order. $X_1$, $X_2$ and $X_3$ are, respectively, the coded scale factors of the studied parameters.

The calculation of the coefficients of the mathematical model using a Nemrodw software was used to determine the individual effects and interaction effects of the three parameters on the response (Table 2). Analysis of results according to Pareto [7] (Fig. 3) has also allowed to identify the most influential factors.

Thus, to improve the adsorption capacity of the two dyes on RL, it has been shown that:

- mass of lignin and contact time must be increased since their coefficients are positive,
- initial concentration of dyes must be decreased, its coefficient is negative,
- interactions between factors are low and
- mass of lignin is the most important factor (as given in bold in Table 2).

In addition, results show that the amount of adsorbed dye at equilibrium is as much important that the amount of lignin is high. This behavior is likely due to the number of

Table 1
Matrix of experiment $2^3$ and studied response ($R$%)

| Experiment | Mass of the adsorbent (mg) | Concentration of the adsorbate (mg/L) | Contact time (min) | Retention rate $R$% | |
|---|---|---|---|---|---|
| | | | | MB | MO |
| 1 | 10 (–1) | 5 (–1) | 5 (–1) | 27 | 25 |
| 2 | 50 (+1) | 5 | 5 | 73 | 62 |
| 3 | 10 | 10 (+1) | 5 | 18 | 17 |
| 4 | 50 | 10 | 5 | 41 | 35 |
| 5 | 10 | 5 | 30 (+1) | 23 | 18 |
| **6** | **50** | **5** | **30** | **80** | **78** |
| 7 | 10 | 10 | 30 | 21 | 15 |
| 8 | 50 | 10 | 30 | 58 | 57 |

Table 2
Coefficients of the factors affecting the adsorption of dyes on raw lignin

| Name | Coefficients | |
|---|---|---|
| | MB | MO |
| Average ($b_0$) | 41.125 | 38.375 |
| **Mass of the lignin (b1)** | **20.375** | **19.625** |
| Concentration of dyes ($b_2$) | –7.625 | –7.375 |
| Stirring time ($b_3$) | 2.875 | 3.625 |
| Mass–concentration ($b_{12}$) | –5.375 | –4.625 |
| Mass–stirring time ($b_{13}$) | 3.125 | 5.875 |
| Concentration–stirring time ($b_{23}$) | 2.125 | 1.375 |
| Mass–concentration–stirring time ($b_{123}$) | 0.375 | 0.125 |

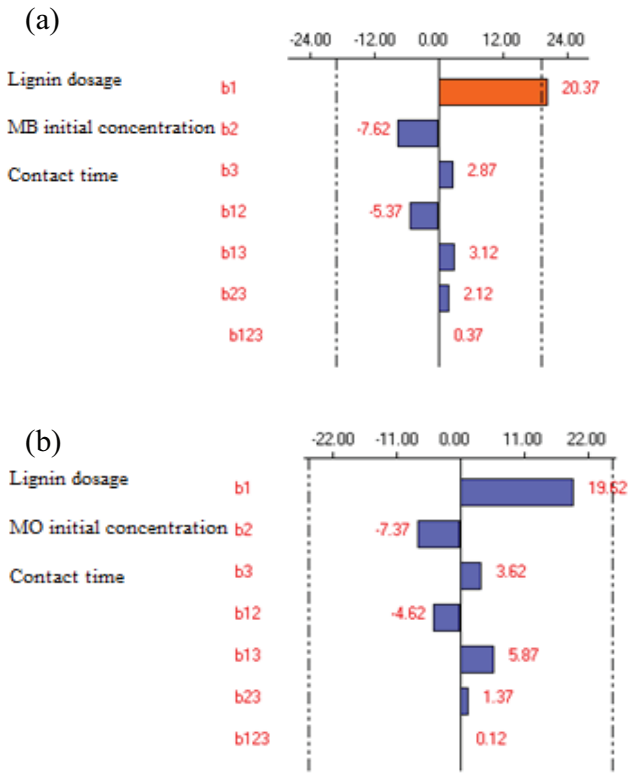


Fig. 3. Pareto diagram of the adsorption of MB (a) and MO (b) on RL.

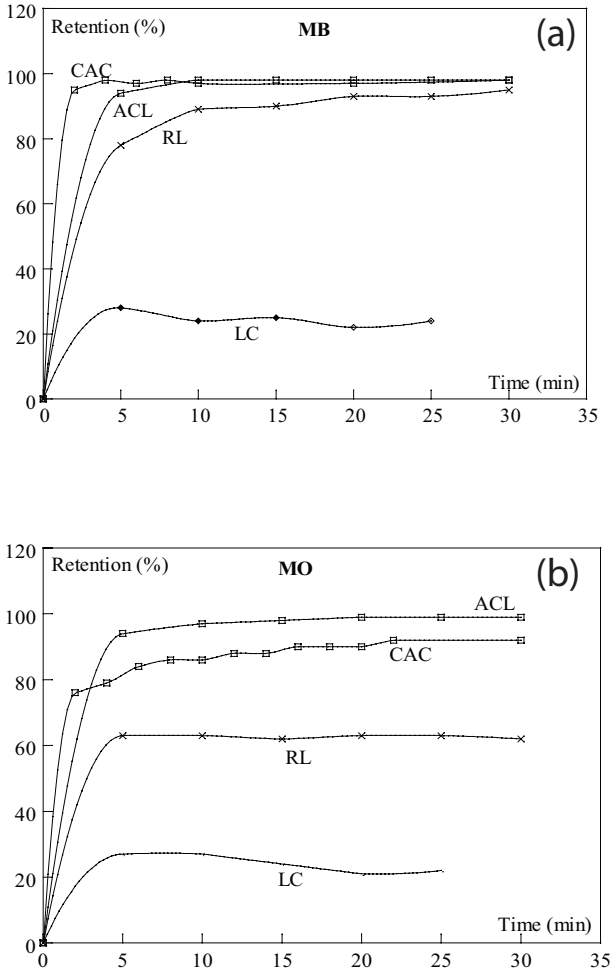


Fig. 4. Adsorption of MB (a) and MO (b) on RL, LC, ACL and CAC.

Table 3
Retention rate and equilibrium time of the different materials in the case of MB and MO

| Adsorbent | | RL | LC | ACL | CAC |
|---|---|---|---|---|---|
| Retention rate (%) | MB | 95 | 24 | 98 | 98 |
| Equilibrium time (min) | | 10 | 20 | 5 | 5 |
| Retention rate (%) | MO | 60 | 23 | 97 | 90 |
| Equilibrium time (min) | | 5 | 20 | 5 | 22 |

active sites available on the surface of the lignin is particularly important that the mass used is large, which facilitates the adsorption of significant quantities of the dye.

### 3.2. Adsorption kinetics

Fig. 4 summarizes the results of adsorption kinetics of MB and MO on RL, its derivative charcoals and CAC. Maximum retention rates and equilibrium time deduced from the different curves are grouped in Table 3. The same figure shows that the general shape of the kinetic curves is almost the same and it takes place in two stages. The first corresponds to a very rapid increase in the retention rate in the first minutes and the second is relative to a slow increase until it reaches a steady state. The first would be linked to the fixation of the adsorbate on the easily accessible sites and the second to the distribution thereof to the less accessible sites until all sites are occupied.

As regards the RL, MB is better adsorbed than MO (Table 3). This would indicate that the acid sites are more numerous than the basic sites. Moreover, this result is corroborated by the measurement of the surface charge carried out on RL. Indeed, the surface of the lignin is negatively charged because the $pH_{PZC}$ is 2.25 while the initial pH value is 6.25 (section 2.3.3, Fig. 2). For LC, the adsorption of MB and MO

are equivalent. Under these conditions, the number of basic sites is equivalent to the number of acid sites. For the two dyes, adsorption on LC is significantly lower than on RL. This is due to the elimination of sites that favored the adsorption, the formation and the development of the thermoplastic nature of LC during carbonization [1].

As in the case with LC, adsorption of MB and that of MO on ACL are equivalent. This is due to the fact that ACL contains as many acid sites as basic sites. On the other hand, with ACL, adsorption of MB and MO are higher than those on LC and RL (Table 3). Activation of LC reduces its thermoplastic character and improves its physico-chemical characteristics as shown in specific surface area measurements and surface functional groups [1,2]. Indeed, reduction of the thermoplastic nature of LC is revealed by transmission electron microscopy (Fig. 5). As for the measures of specific surfaces, they show that LC has a surface area much smaller than those of RL and ACL (Table 4). Finally, infrared spectroscopy reveals that the functional groups involved in the adsorption phenomena are present in the RL and in its activated carbon (ACL) but not in its carbonized form (LC). These functional groups could be carbonyl groups (Fig. 6). The above interpretations explain the low retention rate of LC (Table 3).

It is possible from the adsorption tests to note that RL contains more acid sites than basic sites. The number of these two types of sites decreases considerably after carbonization and the little that remains is equivalent. The number of these

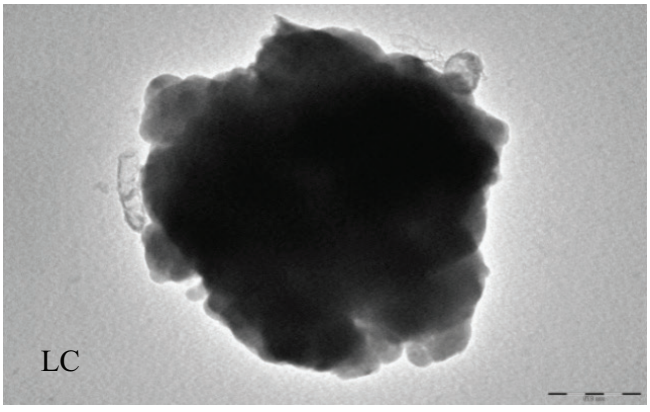


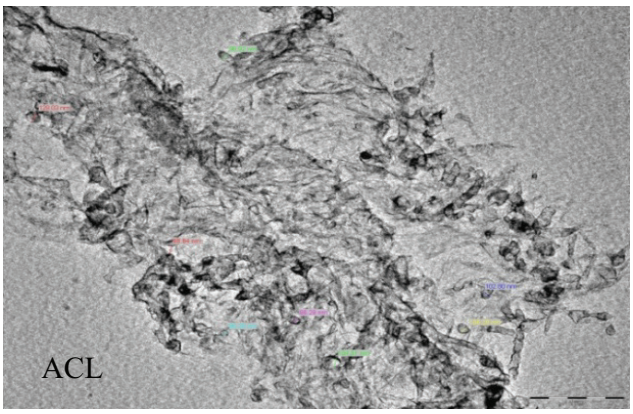


Fig. 5. TEM images of the derivative charcoals of lignin.

Table 4
Specific surface areas of raw lignin and its derivative charcoals

| Sample | Specific surface area ($m^2/g$) |
|---|---|
| RL | 180 |
| LC | 32.45 |
| ACL | 394.26 |

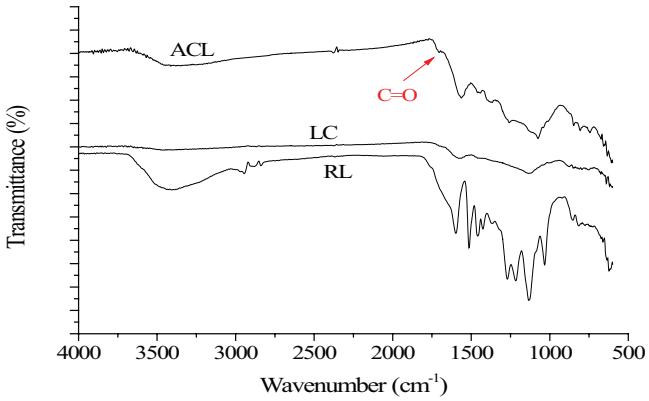


Fig. 6. Infrared spectra of raw lignin and its derivative charcoals.

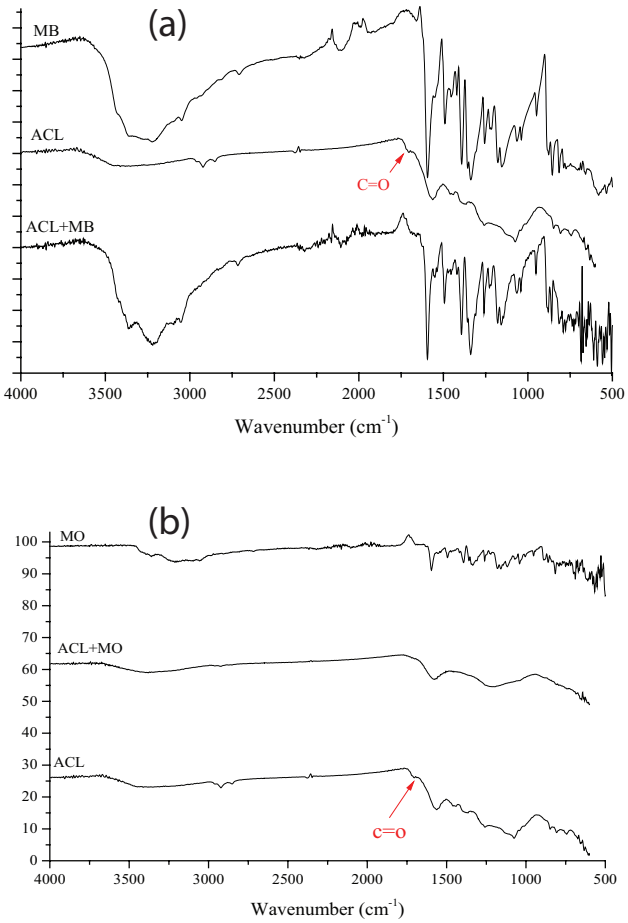


Fig. 7. IR spectra of ACL before and after adsorption of MB (a) and MO (b).

two types of sites increases after activation without reaches that of the RL while remaining equivalent.

Furthermore, adsorption of MB on ACL is practically equivalent to that on CAC. Thus, the two adsorbents have the same number of acid sites. On the other hand, adsorption of MO on ACL is more important than on CAC. Under these conditions, the number of basic sites of ACL is greater than that of CAC (Table 3).

From the results of Table 3, equilibrium time of MO on RL is the same as on ACL but retention rate has been improved by about 40%. Retention rate of MB on RL is practically equivalent to that on ACL but equilibrium time has been reduced by about 50%.

Infrared characterization confirms the adsorption of MB and MO on ACL. Indeed, the spectrum related to ACL after adsorption of MB shows the presence of characteristic bands of MB in addition to those of ACL (Fig. 7(a)). As for the IR spectrum of ACL after adsorption of MO, the corresponding absorption bands are lower than those of ACL before adsorption. This is due to the amorphous character of MO (Fig. 7(b)).

### 3.3. Kinetic models

In order to explore the mechanism involved in adsorption process of MB and MO on RL and ACL and to deduce

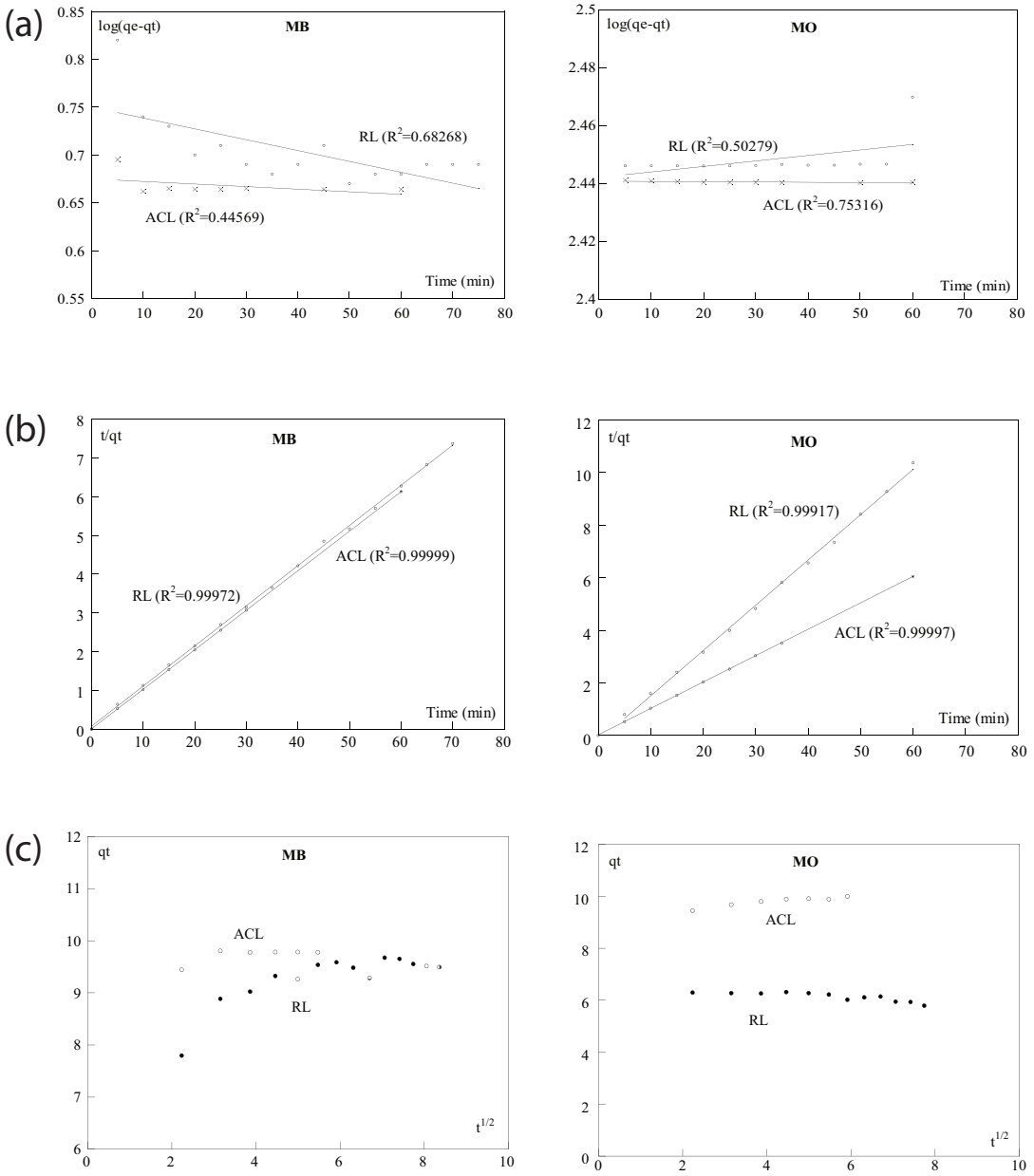


Fig. 8. Adsorption kinetic models of pseudo-first order (a), pseudo-second order (b) and intraparticle diffusion (c) of MB and MO on RL and ACL.

Table 5
Parameters of kinetic models

| Kinetic models | Parameters | Adsorbent/adsorbate | | | |
|---|---|---|---|---|---|
| | | RL | | ACL | |
| | | MB | MO | MB | MO |
| Pseudo-first order | $R^2$ | 0.68268 | 0.50279 | 0.44569 | 0.75316 |
| Lagergren model [9] | $k_1$ (min$^{-1}$) | 0.00262 | 0.00044 | 0.000611 | $2.669 \times 10^{-5}$ |
| | $q_e$ (mg/g) | 5.6247 | 276.885 | 4.7298 | 276.058 |
| $\log(q_e - q_t) = \log q_e - \frac{k_1}{2{,}303} t$ (3) | | | | | |
| Pseudo-second order | $R^2$ | 0.99972 | 0.99917 | 0.99999 | 0.99997 |
| Ho and Mckay model [10] | $k_2$ (g/mg min) | 0.1489 | 0.1389 | 2.2358 | 0.5785 |
| | $q_{e\,\text{theo}}$ (mg/g) | 9.646 | 5.811 | 9.7895 | 9.9611 |
| $\frac{t}{q_t} = \frac{1}{k_2 q_e^2} + \frac{t}{q_e}$ (4) | $q_{e\,\text{exp}}$ (mg/g) | 9.66 | 6.28 | 9.78 | 9.91 |
| | $\Delta q = q_{e\,\text{theo}} - q_{e\,\text{exp}}$ (mg/g) | 0.014 | 0.469 | 0.0095 | 0.0511 |
| Intraparticle diffusion | $R^2$ | – | 0.85667 | 0.69382 | 0.95117 |
| Weber and Morris model [11] | $k_d$ (mg/g min$^{1/2}$) | – | 0.08477 | 0.08037 | 0.13447 |
| | $I$ | – | 6.5854 | 9.3989 | 9.2138 |
| $q_t = k_d t^{1/2} + I$ (5) | | | | | |

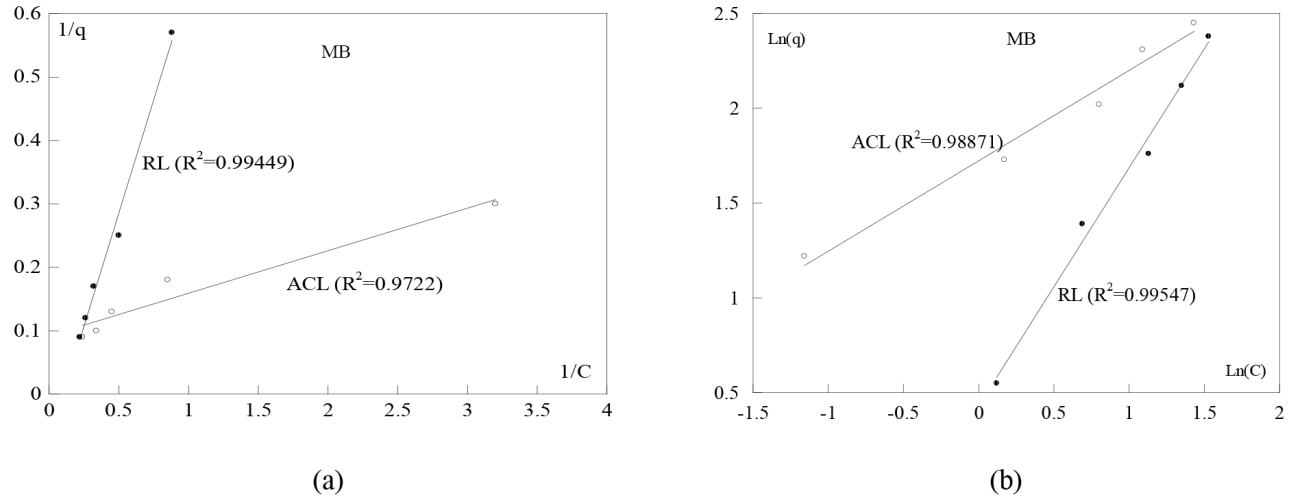


Fig. 9. Langmuir (a) and Freundlich (b) isotherms for adsorption of MB on RL and on ACL.

limiting step for this process [8], the models of pseudo-first order, pseudo-second order and intraparticle diffusion are applied. Results of this modeling are shown in Fig. 8 and values of the correlation coefficients as well as the mathematical expression of each model and the corresponding kinetic parameters deduced from the slope and intercept at the origin of the different curves are grouped in Table 5.

With $q_t$ and $q_e$: quantities of adsorbate per unit mass of adsorbent, respectively, at a time $t$ and at equilibrium time (mg/g); $t$: contact time (min); $k_1$, $k_2$ and $k_d$: rate constants, respectively, for kinetic equation of pseudo-first order (min$^{-1}$), pseudo-second order (g/mg min) and intraparticle diffusion (mg/g min$^{1/2}$); I: interception (mg/g).

Examination of Fig. 8 shows that for the two adsorbates and the two adsorbents, the pseudo-second order model well describes the experimental data (Fig. 8(b)) especially as the corresponding correlation coefficient is higher than those of the other two models (Table 5). In addition, adsorbed amounts at equilibrium calculated by pseudo-second order model are consistent with those obtained experimentally (Table 5). These two conditions would indicate that the adsorption process is mainly controlled by chemisorption [12,13]. According to Ho [14],

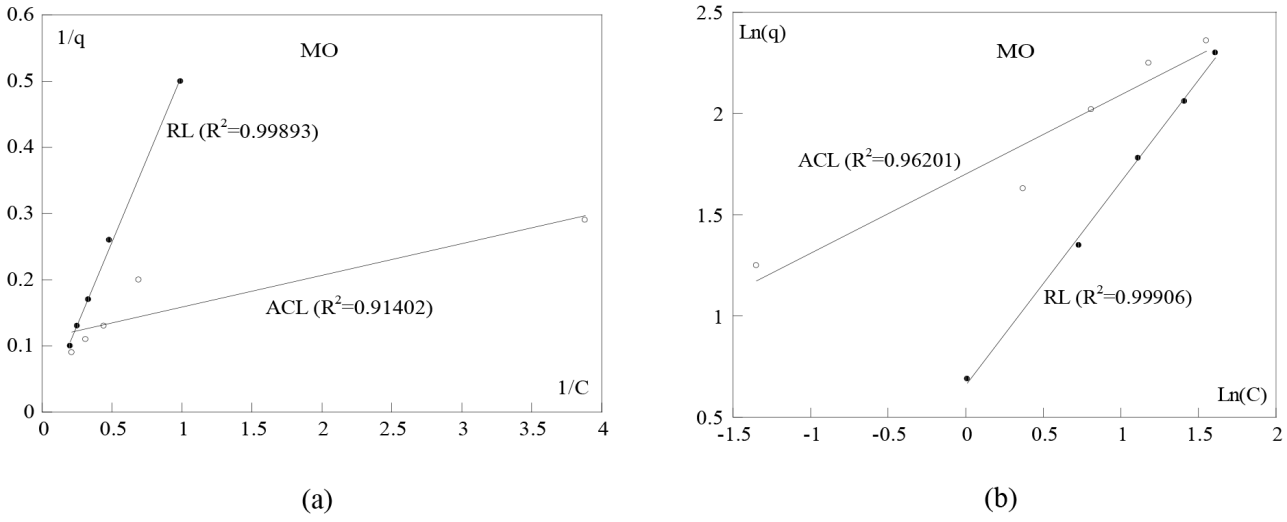


Fig. 10. Langmuir (a) and Freundlich (b) isotherms for adsorption of MO on RL and on ACL.

Table 6
Constants of Langmuir and Freundlich models

| Adsorbent | Adsorbate | Adsorption isotherms | | | | | | | | |
|---|---|---|---|---|---|---|---|---|---|---|
| | | Langmuir $\frac{1}{q}=\frac{1}{q_m}+\frac{1}{q_m k_L}\frac{1}{C}$ (6) | | | | | Freundlich $\mathrm{Ln}(q)=n\mathrm{Ln}(C)+\mathrm{Ln}(k_F)$ (7) | | | |
| | | $R^2$ | $q_{m\,\mathrm{cal}}$ | $q_{m\,\mathrm{exp}}$ | $K_L$ | $R_L$ | $R^2$ | $n$ | $1/n$ | $K_F$ |
| RL | MB | 0.99449 | 14 | 9.67 | 0.1 | 0.5 | 0.99547 | 1.2555 | 0.7965 | 1.54 |
| | MO | 0.99893 | 194.88 | 6.31 | 0.01 | 0.91 | 0.99906 | 1.004 | 0.9960 | 1.93 |
| ACL | MB | 0.9722 | 10.887 | 9.80 | 1.3695 | 0.068 | 0.98871 | 0.47627 | 2.0996 | 5.61 |
| | MO | 0.91402 | 9.003 | 9.99 | 2.3211 | 0.041 | 0.96201 | 0.39133 | 2.5554 | 5.48 |

where $q$ and $q_m$ are the adsorbed amount at equilibrium and the maximum amount absorbed per unit mass of the adsorbent (mg/g), respectively, $C$ is the residual equilibrium concentration (mg/L); $n$, $1/n$, $K_L$ and $K_F$ are the parameter of Freundlich, the factor of heterogeneity, the Langmuir constant (L/mg) and the Freundlich constant related to the adsorption capacity ($mg^{(1-n)}L^n/g$), $R_L$ is the dimensionless constant called separation factor or parameter of equilibrium.

chemisorption is related to polar functional groups of lignin, including the carboxyl groups, which are involved as chemical bonding agents. Other authors [15–17] consider that chemisorption involves valence forces by the sharing or exchange of electrons between adsorbent and adsorbate. The intraparticle diffusion does not represent the rate-limiting step because the curves of the different adsorbent/adsorbate systems do not pass through the origin (Fig. 8(c)). However, in the case of RL/MB, we have a two/tri-linearity. The adsorption of MB onto RL takes two or three steps.

### 3.4. Adsorption isotherms

Linear representations of the experimental values of MB and MO adsorption on RL and on its activated carbon by Langmuir [18] and Freundlich [19] models are given in Figs. 9 and 10, the correspondent parameters are summarized in Table 6. Parameters of discrimination are the correlation coefficient and the amount adsorbed.

For RL, the values of correlation coefficients are close to 1 for the two isotherms. Thus, adsorption of the two dyes on RL appears to follow Langmuir model as well Freundlich one. But since adsorbed quantity of MO calculated by Langmuir model differs greatly from the experimental value (Table 6), Langmuir model so not describes satisfactorily the experimental data. Thus, Freundlich model is the most adequate to describe adsorption of MB and MO on RL.

For ACL, the values of correlation coefficients (Table 6) show that Freundlich model is most suitable for the two adsorbates. Thus, adsorption of MB and MO on RL and its activated carbon is done in multilayers on heterogeneous surfaces.

For both dyes and in considering the values of $n$ (Table 6), adsorption is more important on ACL compared with RL. Indeed, the specific surface area of ACL is

higher than that of RL (Table 4). In addition, carbonyl group involved in adsorption has a greater intensity on the infrared spectrum for ACL than RL.

As regards $1/n$, its value is less than 1 in the case of RL and greater than 1 in the case of ACL. Freundlich isotherm is then normal in the first case and cooperative in the second.

## 4. Conclusion

From this work, we have concluded that equilibrium time of MO on RL is the same as that on its activated carbon but the retention rate has been improved by about 40%. Retention rate of MB on RL is practically equivalent to that on its activated carbon but equilibrium time has been reduced by about 50%. Otherwise, adsorption of MB on ACL is practically equivalent to that on CAC, while MO adsorption on ACL is more important than on CAC. Chemisorption governs adsorption of the two dyes both on RL and on its activated carbon. In addition, the two dyes are adsorbed in multilayers on heterogeneous surfaces.

## References

[1] S. Sebbahi, F. Kifani-Sahban, S. El Hajjaji, A. Zoulalian, Pré-oxydation et activation du charbon de la lignine: Procédure de l'activation, Bull. Soc. R. Sci. Liège, 40 (2015) 194–206.
[2] S. Sebbahi, L. El Fakir, L. Rghioui, A. El Hajji, Y. Brik, F. Kifani-Sahban, S. El Hajjaji, Characterization of lignin and derivative chars by infrared spectroscopy, J. Mater. Environ. Sci., 6 (2015) 2461–2468.
[3] F. Kifani-Sahban, A. Kifani, L. Belkbir, A. Zoulalian, J. Arauso, T. Cordero, A physical approach in the understanding of the phenomena accompanying the thermal treatment of lignin, Thermochim. Acta, 298 (1997) 199–204.
[4] S. Chatterjee, S. Chatterjee, B.P. Chatterjee, A.R. Das, A.K. Guha, Adsorption of a model anionic dye, eosin Y, from aqueous solution by chitosan hydrobeads, J. Colloid Interface Sci., 288 (2005) 30–35.
[5] L. El Fakir, M. Flayou, A. Dahchour, S. Sebbahi, F. Kifani-Sahban, S. El Hajjaji, Adsorptive removal of copper (II) from aqueous solutions on phosphates: equilibrium, kinetics, and thermodynamics, Desal. Wat. Treat., 57 (2016) 17118–17127.
[6] A. El Yadini, M. El Azzouzi, L. El Fakir, B. Birich, P. Schmitt–Kopplin, M. Harir, S. El Hajjaji, Etude de l'influence de différents paramètres sur la dégradation du phénamiphos en milieux aqueux par la méthodologie de la recherche expérimentale, Sci. Liberté, 5 (2013) 1–12.
[7] D. Mathieu, R. Phan-Tan-Luu, NEMROD®, SoftwareLPRAI, Marseille, France, 1995.
[8] D. Robati, Pseudo-second-order kinetic equations for modeling adsorption systems for removal of lead ions using multi walled carbon nanotube, J. Nanostruct. Chem., 3 (2013) 1–6.
[9] S. Lagergren, Zur theorie der sognenannten adsorption gelöster stoffe, K. Sven. Vetensk.akad. Handl., 24 (1898) 1–39.
[10] Y.S. Ho, G. Mckay, Pseudo second order model for sorption processes, Process Biochem., 34 (1999) 451–465.
[11] W.J. Weber, J.C. Morris, Kinetic of adsorption on carbon from solution, J. Sanitary Eng. Div. Proc. Am. Soc. Civil Eng., 89 (1963) 31–60.
[12] Y.S. Ho, G. Mckay, A comparison of chemisorption kinetic models applied to pollutant removal on various sorbents, Process Saf. Environ. Prot., 76 (1998) 332–340.
[13] Y.S. Ho, G. Mckay, The kinetics of sorption of divalent metal ions onto sphagnum moss peat, Water Res., 34 (2000) 735–742.
[14] Y.S. Ho, Removal of copper ions from aqueous solution by tree fern, Water Res., 37 (2003) 2323–2330.
[15] D. Mohan, K.P. Singh, V.P. Singh, Trivalent chromium removal from wastewater using low cost activated carbon derived from agricultural waste material and activated carbon fabric cloths, J. Hazard. Mater., 135 (2006) 280–295.
[16] I. Kula, M. Uqurlu, H. Karaoglu, A. Celik, Adsorption of Cd(II) ions from aqueous solutions using activated carbon prepared from olive stone by $ZnCl_2$ activation, Bioresour. Technol., 99 (2008) 492–501.
[17] P.J. Suhas, M.M. Carrott, C. Ribeiro, Lignin from natural adsorbent to activated carbon: a review, Bioresour. Technol., 98 (2007) 2301–2312.
[18] I. Langmuir, The adsorption of gases on plane surfaces of glass, mica and platinum, J. Am. Chem. Soc., 40 (1918) 1361–1403.
[19] H.M.F. Freundlich, Over the adsorption in solution, J. Phys. Chem., 57 (1906) 385–470.